Article

Generalized Geometric Interpretation of Temperature Control for Ternary Distillation

Michael L. Luyben, Min-Te Lin, Jian-Kai Cheng, and Cheng-Ching Yu

More About This Article

Additional resources and features associated with this article are available within the HTML version:

- Supporting Information
- Access to high resolution figures
- Links to articles and content related to this article
- Copyright permission to reproduce figures and/or text from this article

View the Full Text HTML

Generalized Geometric Interpretation of Temperature Control for Ternary Distillation

Michael L. Luyben,[†] Min-Te Lin,[‡] Jian-Kai Cheng,[‡] and Cheng-Ching Yu*,[‡]

E. I. du Pont de Nemours & Co., Inc., 1007 Market St.−B7434, Wilmington, Delaware 19898, and Department of Chemical Engineering, National Taiwan University, Taipei 106-17, Taiwan

A previous paper introduced the concept of traveling distance to quantify how much the composition profile in a distillation column has to change when certain tray temperatures are held constant under single-end temperature control. The larger the traveling distance for a given temperature-control selection, the slower the composition dynamics and, hence, the poorer the control performance are expected to be. This work generalizes the concept of traveling distance in distillation-temperature control for different levels of complexity in a ternary distillation column separating components A, B, and C, in order of decreasing volatility. For the *direct* separation between A and B/C with a high purity of A at the top, the analysis shows that the conflict between process and control direction becomes more severe (larger traveling distance) with (1) increasing overhead purity of A, (2) decreasing relative volatility between light and heavy key components (A and B, respectively), (3) increasing relative volatility between the heavy and heavier-than-heavy key components (B and C, respectively), and (4) decreasing feed composition of the light key component (A). The results can be inverted to the indirect separation between A/B and C with a high purity of C at the bottom, while substituting heavy for light in the above conclusions.

1. Introduction

In a previous paper (Lin et al.[1]), we proposed a geometric interpretation of distillation column temperature control in the triangular composition space for a ternary system. We examined a specific column design with components of a certain assumed constant relative volatility as a way to illustrate the basic concepts concerning the choice of control-tray temperature.

In spite of the many advances in the technology to have direct, fast on-line measurement of product purities, the controlled variable for product quality in many industrial distillation columns is tray temperature. Many approaches have been proposed over the decades for selecting the proper temperature-control points and for composition estimation in distillation columns.[2−11] Our previous paper explained physically why certain temperature locations are superior to others, particularly in ternary (or multicomponent) columns. We considered a general three-component mixture of A, B, and C in order of decreasing volatility. If we assume constant relative volatility, then isotherms in the triangular composition space are straight lines with a slope directly proportional to the ratio of relative volatilities of components A and B.

We showed the interaction between the direction of the process composition profile in triangular space to achieve the desired component separation and the direction of the control composition profile to maintain a constant tray temperature. A potential conflict can arise between the process and control directions. The traveling distance can be used as a quantitative measure to calculate how much the column composition profile must change with certain tray temperatures held constant. The traveling distance can be computed from steady-state gain matrices but provides useful dynamic information about control performance. The larger the value of the traveling distance for
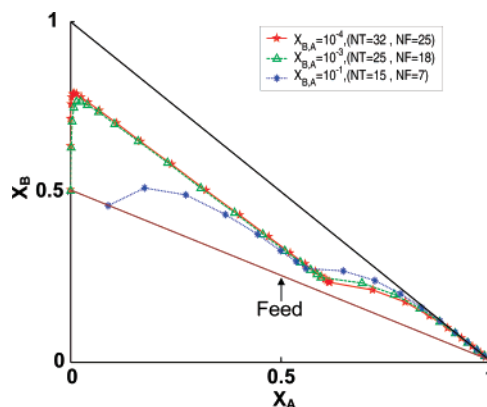
Figure 1. Steady-state composition profiles for different bottoms product purities and the material balance line (feed and top and bottoms product composition) also indicated in the ternary composition space.

a given temperature-control selection, the slower the composition dynamics and, hence, the poorer the control performance is expected to be.

The objective of this paper is to generalize these concepts on the temperature control of multicomponent distillation columns by studying design parameters for (1) different product purity levels, (2) different relative volatilities between A/B and B/C, (3) different feed compositions, and (4) different separation structures (direct split and indirect split).

2. Effects of Product Purities

Here we look at how product-purity levels affect the column temperature control. Because of process nonlinearity, control of a high-purity distillation column has received some attention in the past.[11−15] Here, we want to determine whether the traveling distance can be used as a measure of the expected temperature-control performance (e.g., speed of response) as the product-purity specifications become more severe. Our results from the linearized transfer functions will be validated via nonlinear dynamic simulation.

* Corresponding author. Tel.: +886-2-3366-3037. Fax: +886-2-2362-3040.
† E. I. du Pont de Nemours & Co., Inc.
‡ National Taiwan University.

Table 1. Steady-State Operating Conditions for Different Product Purities

	base case ($X_{B,A} = 10^{-3}$)	$X_{B,A} = 10^{-1}$	$X_{B,A} = 10^{-4}$
F (mol/h)	45.4	45.4	45.4
R (mol/h)	49.5	42.9	52.3
RR	2.15	2.06	2.27
B (mol/h)	22.3	24.5	22.4
D (mol/h)	23.0	20.9	23.0
V (mol/h)	72.7	63.8	75.3
N_T	25	15	32
N_F	18	7	25
$\alpha_A/\alpha_B/\alpha_C$	4/2/1	4/2/1	4/2/1
β (s)	3.2	2.9	3.2
$M_B/M_D/M_N$ (mol)	7.9/6.0/0.3	6.8/6.5/0.3	8.1/6.3/0.3
$Z_A/Z_B/Z_C$ (m.f.)	0.5/0.256/0.244	0.5/0.256/0.244	0.5/0.256/0.244
$X_{D,A}/X_{D,B}/X_{D,C}$ (m.f.)	0.982/0.0175/0.0005	0.981/0.018/0.001	0.9859/0.014/0.0001
$X_{B,A}/X_{B,B}/X_{B,C}$ (m.f.)	0.001/0.503/0.496	0.009/0.459/0.451	0.001/0.505/0.494
$A_{vp,A}/A_{vp,B}/A_{vp,C}/B_{vp}^*$	15.2/14.5/13.8/−2768.55	15.2/14.5/13.8/−2768.55	15.2/14.5/13.8/−2768.55
normal B.P. (K) (A/B/C)	323.2/351.6/385.5	323.2/351.6/385.5	323.2/351.6/385.5

[a] $\ln P_i^{sat} = A_{vp,i} + (B_{vp})/(T)$, where T is in Kelvin.

2.1. Process Description. We consider first the direct split where component A goes overhead and components B and C go out the bottom of the column. So component A is the light key (LK), component B is the heavy key (HK), and component C is the heavier-than-heavy key (HHK). Three different values of bottoms product purity were studied with a fixed feed composition. The composition or mole fraction of impurity A in the bottoms ($X_{B,A}$) is varied with about the same constant distillate mole fraction of A ($X_{D,A}$). For a given base composition, the column is redesigned by assuming a reflux ratio that is 1.2 times the minimum. This varies the reflux ratio, the total number of theoretical stages, and the feed stage. A value of $X_{B,A}$ of 10^{-3} is the base case, whereas $X_{B,A}$ of 10^{-4} moves the composition profile closer to the edge of the triangular diagram and $X_{B,A}$ of 10^{-1} moves it away from the edge. Table 1 gives the steady-state designs and operating conditions for these three alternatives. Figure 1 shows that, as $X_{B,A}$ increases (impurity A increases), the composition profile moves away from the B−C edge.

2.2. Temperature Control. In this work, single-end temperature is studied. If the bottoms product composition is of interest, we use reboiler duty to maintain a tray temperature in the stripping section as shown in Figure 2. If the top composition is of interest, the reflux flow rate is used to maintain a tray temperature in the rectifying section. Also notice here that the proposed traveling distance approach can be extended to multivariable control in a straightforward manner.[1]

2.3. Dynamics. The potential temperature-control trays for each of the three designs can be selected according to a sensitivity analysis looking at reboiler duty (Figure 3), or we can look at using the first theoretical stage from the bottom (T_1) for temperature control. Note that, in this work, we count the tray number from bottoms upward with the column base as tray zero. The results of the sensitivity analysis are as follows:

$$X_{B,A} = 10^{-1}: T_2 \text{ (most sensitive tray, Figure 3A)}$$

$$X_{B,A} = 10^{-3}: T_{10} \text{ (most sensitive tray, Figure 3B)}$$

$$X_{B,A} = 10^{-4}: T_{13} \text{ (most sensitive tray, Figure 3C)}$$

The traveling distance is defined as the change in composition profile needed with tray temperatures held con-

stant.[1] It can be derived from the linearized open-loop transfer function

$$\begin{bmatrix} x_{1,1} \\ \vdots \\ x_{NT,1} \\ x_{1,2} \\ \vdots \\ x_{NT,2} \\ T_1 \\ \vdots \\ T_{NT} \end{bmatrix} = \begin{bmatrix} G_{1,1} \\ \vdots \\ G_{NT,1} \\ G_{1,2} \\ \vdots \\ G_{NT,2} \\ G_{T1} \\ \vdots \\ G_{TNT} \end{bmatrix} [u] + \begin{bmatrix} G_{L1,1} \\ \vdots \\ G_{LNT,1} \\ G_{L1,2} \\ \vdots \\ G_{LNT,2} \\ G_{LT1} \\ \vdots \\ G_{LTNT} \end{bmatrix} [d] \qquad (1)$$

where $x_{j,i}$ is molar fraction of the component i of the jth tray, T_j is the temperature of the jth tray, $G_{j,i}$ denotes the process transfer function of the component i of the jth tray, G_{Tj} is the process transfer function of the jth temperature control tray, $G_{Lj,i}$ stands for the load transfer function of the component i of the jth tray, G_{LTj} is the load transfer function of the jth temperature-control
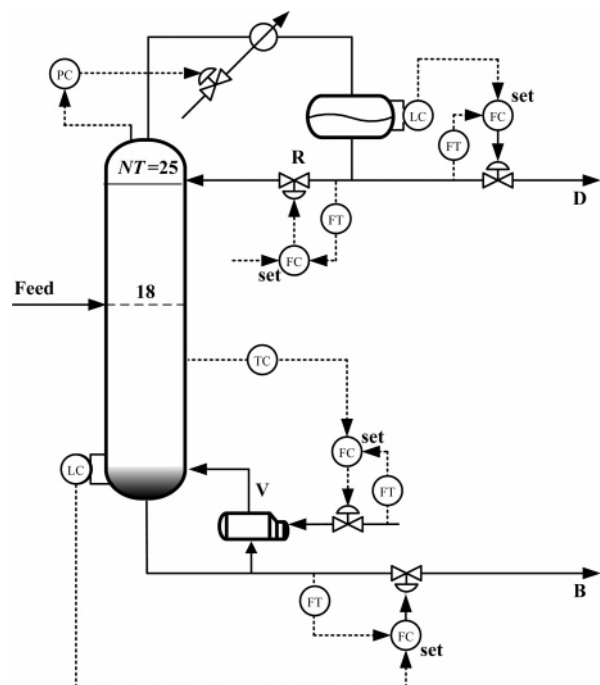
Figure 2. Control a tray temperature in the stripping section using reboiler duty while keeping the reflux flow rate constant.
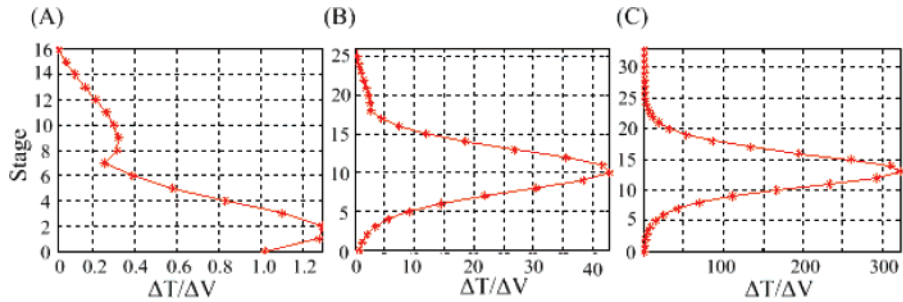
Figure 3. Sensitivity analysis to heat input change when (A) $X_{B,A} = 10^{-1}$, (B) $X_{B,A} = 10^{-3}$, and (C) $X_{B,A} = 10^{-4}$.
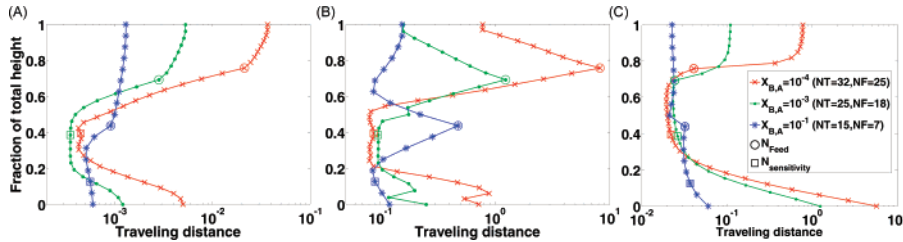

Figure 4. Traveling distance: (A) with F change with different bottoms product purities, (B) with Z_A change for different bottoms product purities, and (C) with Z_B/Z_C change for different product purities. (Note: fractions 0 and 1 correspond to the bottom and top of the column, respectively.)
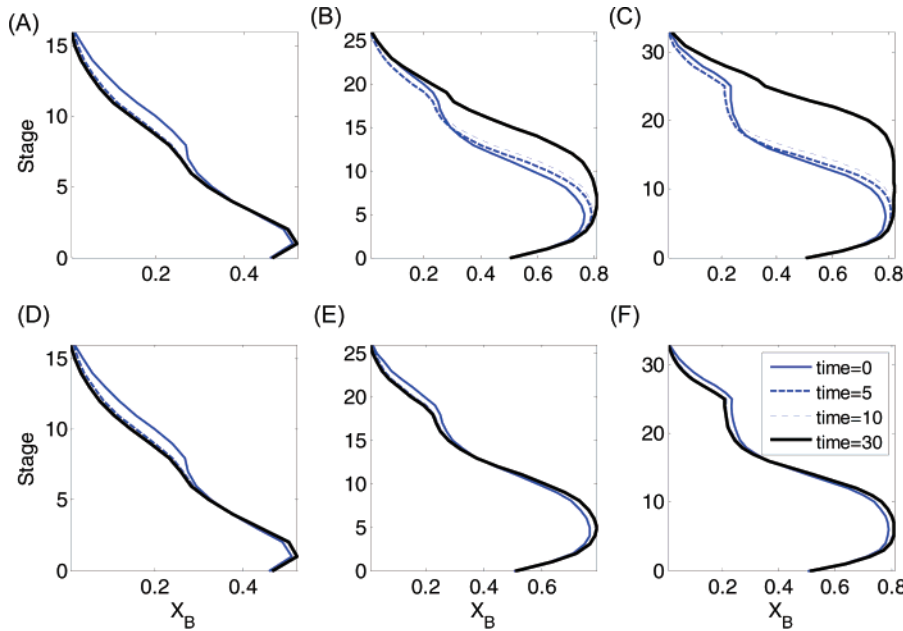

Figure 5. Snapshots of composition profile of component B for -20% F change with T_1 control when (A) $X_{B,A} = 10^{-1}$, (B) $X_{B,A} = 10^{-3}$, (C) $X_{B,A} = 10^{-4}$, and with $T_{sensitive}$ control when (D) $X_{B,A} = 10^{-1}$, (E) $X_{B,A} = 10^{-3}$, and (F) $X_{B,A} = 10^{-4}$.

tray, u denotes the manipulated variable, and d is the load variable. If T_k is held constant, one obtains

$$
\begin{bmatrix} x_{1,1} \\ \vdots \\ x_{NT,1} \\ x_{1,2} \\ \vdots \\ x_{NT,2} \end{bmatrix} = \begin{bmatrix} G_{L1,1} - G_{1,1}(G_{LTk}/G_{Tk}) \\ \vdots \\ G_{LNT,1} - G_{NT,1}(G_{LTk}/G_{Tk}) \\ G_{L1,2} - G_{1,2}(G_{LTk}/G_{Tk}) \\ \vdots \\ G_{LNT,2} - G_{NT,2}(G_{LTk}/G_{Tk}) \end{bmatrix} [d] \quad (2)
$$

After some algebraic manipulation, the normalized traveling distance becomes

$$
\text{distance}(T_k) = \left[\sum_{j=1}^{NT} \sum_{i=1}^{NC-1} \left(G_{Lj,i} - G_{j,i} \left(\frac{G_{LTk}}{G_{Tk}} \right) \right)^2 \right]^{1/2} / NT \quad (3)
$$

The traveling distance can be computed from the steady-state gain matrices of the process and load transfer functions for a given assumed disturbance involving a change in feed flow (F) shown in Figure 4A, feed composition of component A (Z_A) shown in Figure 4B, or feed composition of components B and C (Z_B/Z_C) shown in Figure 4C. The results clearly show that the traveling distance increases significantly when the purity level increases when T_1 is under control.

Dynamic simulations were also carried out using the most sensitive temperature for control ($T_{sensitive}$) and T_1 as temperature-control trays for the three bottoms purity levels. First, we explore the load responses for a 20% decrease in feed flow. Figure 5 shows the relatively slower dynamic responses observed when T_1 is used for control compared with the response using $T_{sensitive}$ for control. The snapshots of the composition profile of intermediate component B indicate (for T_1 control) that, at time = 30, the profile is far away from the
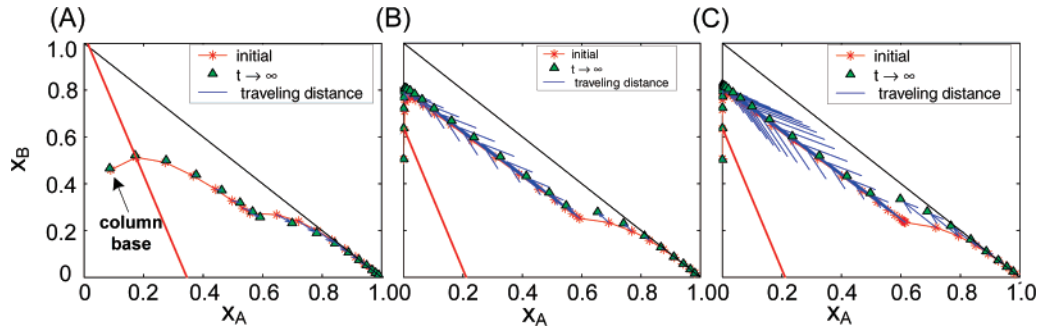
Figure 6. Reshaping composition profile and corresponding traveling distance for T_1 control with -20% F change when (A) $X_{B,A} = 10^{-1}$, (B) $X_{B,A} = 10^{-3}$, and (C) $X_{B,A} = 10^{-4}$ (with the straight line indicating the temperature isotherm, the control direction, and the size of the arrow representing the magnitude and the direction the tray composition traveling, the process direction).
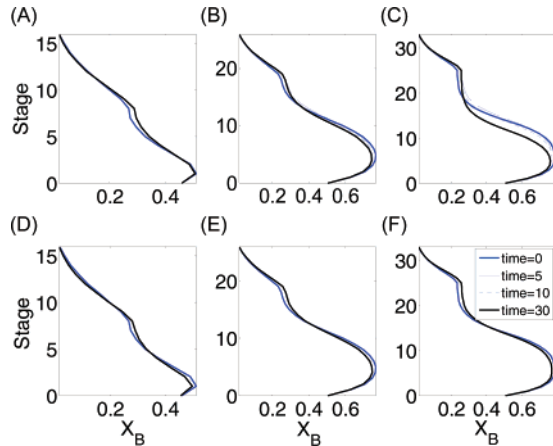
Figure 7. Transient response for -10% Z_A change; $T_1 = $ const: (A) $X_{B,A} = 10^{-1}$, (B) $X_{B,A} = 10^{-3}$, and (C) $X_{B,A} = 10^{-4}$; $T_{\text{sensivity tray}} = $ constant: (D) $X_{B,A} = 10^{-1}$, (E) $X_{B,A} = 10^{-3}$, and (F) $X_{B,A} = 10^{-4}$.

final steady state. The difference between $t = 30$ and $t = $ infinity gets larger as the bottoms purity increases. Figure 6 shows that the traveling distance, as indicated by the arrows in the composition space, goes up quickly when the bottoms composition becomes more pure.

Second, Figure 7 shows the profiles of component B when the feed composition of A decreases by 10%. The traveling distance increases moderately when T_1 is under control, but little difference in the distances is observed if the most sensitive tray is held constant. Third, we examine a 10% decrease in the feed composition of component B (based on the feed mole fraction ratio Z_B/Z_C). The results of dynamic simulation show that T_1 temperature control is much slower than the $T_{\text{sensitive}}$ control, especially for the high purity case. Moreover, little change in the composition profile is observed when the most sensitive tray is under temperature control. This is due to a significant traveling distance for T_1 control and the fact that the distance increases as the purity goes up.

The conflict between process and control directions will be more severe when the column product purity level increases. Because the composition profile moves closer to the edge of the triangular diagram if $X_{B,A}$ becomes smaller, we essentially lose a degree of freedom for the temperature controller to move the composition profile where it needs to go.

3. Effects of Relative Volatilities

3.1. Process Description. We have so far assumed constant relative volatilities among the three components with relative volatilities of 4/2/1. For the system where A = LK, B = HK, and C = HHK, we can examine how the volatilities affect the

expected control performance. Two cases and four systems are studied. In case 1, we can vary the relative volatility between LK/HK components (α_A/α_B):

Difficult separation: $\alpha_A/\alpha_B/\alpha_C = 3/2/1$

Easy separation: $\alpha_A/\alpha_B/\alpha_C = 8/2/1$

In case 2, we can vary the relative volatility between HK/HHK components (α_B/α_C):

Difficult separation: $\alpha_A/\alpha_B/\alpha_C = 3/1.5/1$

Easy separation: $\alpha_A/\alpha_B/\alpha_C = 8/4/1$

Table 2 gives the steady-state operating conditions for all four cases explored. Figure 8 shows that the slope of the temperature isotherm changes as the relative volatilities between LK/HK and HK/HHK vary. Figure 8A indicates that, relatively speaking, the case of $\alpha_A/\alpha_B/\alpha_C = 3/2/1$ has two distinct disadvantages: (1) it is closer to the X_B-X_C edge and (2) it has the smallest slope in all three cases. Similarly, Figure 8B indicates that, relatively speaking, the case of $\alpha_A/\alpha_B/\alpha_C = 8/4/1$ also has two distinct disadvantages: (1) it is closer to the edge and (2) it has the smallest slope in all three cases. These characteristics indicate potential temperature-control problems if the temperature-control tray is not carefully selected.

3.2. Dynamics. Before we go into the details, the most sensitive temperature control trays for all four cases were selected from sensitivity analyses by changing the reboiler duty. The results are as follows:

Base Case: T_{10} (recall Figure 3)

Case 1

$\alpha_A/\alpha_B/\alpha_C = 3/2/1$: T_{19}

$\alpha_A/\alpha_B/\alpha_C = 8/2/1$: T_3
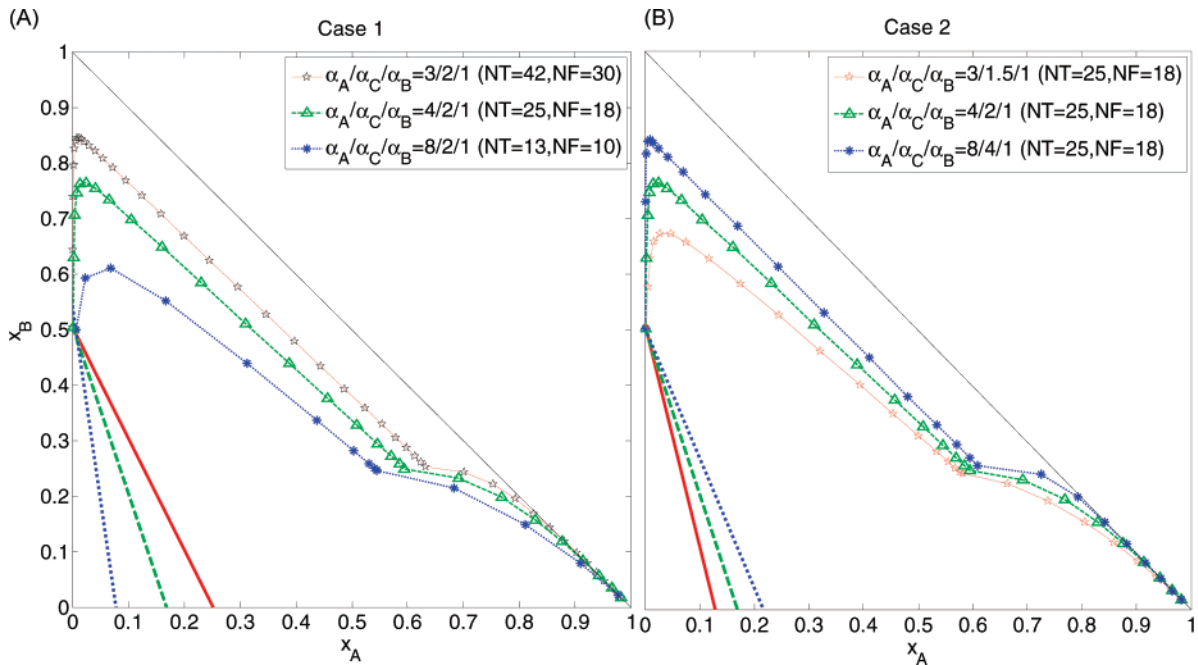
Case 2

$\alpha_A/\alpha_B/\alpha_C = 3/1.5/1$: T_9

$\alpha_A/\alpha_B/\alpha_C = 8/4/1$: T_{11}

Comparisons will be made between temperature control using $T_{\text{sensitive}}$ and T_1.

3.2.1. Traveling Distance for Different Relative Volatilities. First, let us look at case 1 (changing relative volatility between LK/HK). For the Z_B/Z_C disturbance, the $\alpha_A/\alpha_B/\alpha_C = 3/2/1$ case indeed gives the worst-case scenario if T_1 is used for control as

Figure 8. Steady-state composition profiles for different relative volatilities: (A) α_A/α_B change and (B) α_B/α_C change (with the straight lines indicating the corresponding temperature isotherms, when the column base temperature was held constant).
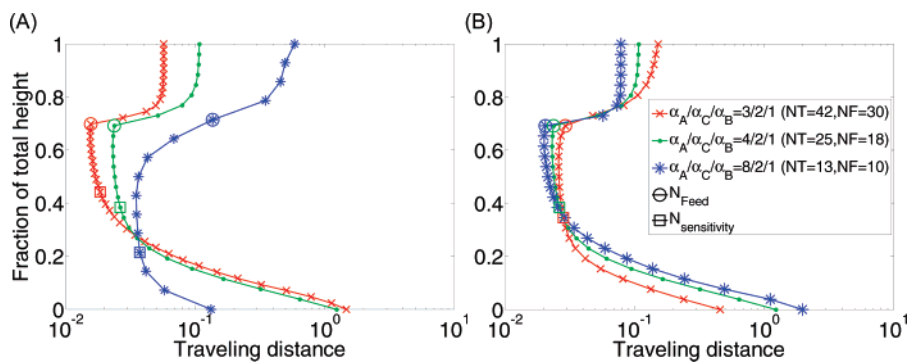
Figure 9. Traveling distance: (A) with Z_B/Z_C change for different α_A/α_B, (B) with Z_B/Z_C change for different α_B/α_C. (Note: fractions 0 and 1 correspond to the bottom and top of the column, respectively.)
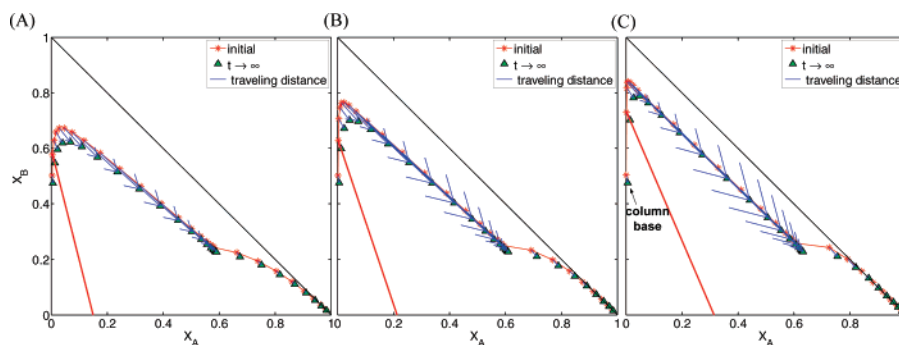
Table 2. Steady-State Operating Conditions for Different Relative Volatilities

	base case	$\alpha_B/\alpha_C = 1.5$	$\alpha_B/\alpha_C = 4$	$\alpha_A/\alpha_B = 1.5$	$\alpha_A/\alpha_B = 4$
$\alpha_A/\alpha_B/\alpha_C$	4/2/1	3/1.5/1	8 /4/ 1	3/2/1	8/2/1
F (mol/h)	45.4	45.4	45.4	45.4	45.4
R (mol/h)	49.5	49.5	49.5	101.4	15.0
RR	2.15	2.06	0.98	4.40	0.65
B (mol/h)	22.3	22.3	22.3	22.3	22.3
D (mol/h)	23.1	23.1	23.1	23.1	23.1
V (mol/h)	72.7	72.7	72.7	124.5	38.0
N_T/N_F	25/18	25/18	25/18	42/30	13/10
β (s)	3.2	3.2	3.2	4.5	2.1
$M_B/M_D/M_N$ (mol)	7.9/6.0/0.3	7.9/6.0/0.3	7.9/6.0/0.3	13.6/10.4/0.4	5.0/3.2/0.1
$Z_A/Z_B/Z_C$ (m.f.)	0.5/0.256/0.244	0.5/0.256/0.244	0.5/0.256/0.244	0.5/0.256/0.244	0.5/0.256/0.244
$X_{D,A}/X_{D,B}/X_{D,C}$ (m.f.)	0.982/0.0175/0.0005	0.981/0.0182/0.0008	0.9828/0.0171/0.0001	0.9826/0.0173/0.0001	0.978/0.021/0.001
$X_{B,A}/X_{B,B}/X_{B,C}$ (m.f.)	0.001/0.503/0.496	0.002/0.503/0.495	0.0005/0.504/0.4955	0.0009/0.5037/0.4954	0.0063/0.4997/0.494
$A_A/A_B/A_C/B^a$	15.2/14.5/13.8/−2768.6	15.2/14.5/14.1/−2768.6	15.2/14.5/13.1/−2768.6	15.2/14.8/14.1/−2768.6	15.2/13.8/13.1/−2768.6
normal B.P. (K) (A/B/C)	323.2/351.6/385.5	323.2/351.6/370.7	323.2/351.6/426.7	323.2/339.2/370.7	323.2/385.5/426.7

^{a} $\ln P_i^{sat} = A_{vp,i} + (B_{vp})/(T)$, where T is in Kelvin.

indicated by the traveling distance in Figure 9A. Similar results can be found for F and Z_A disturbances.[16] Next, we examine case 2 (changing relative volatility between HK/HHK). For the Z_B/Z_C disturbance, the $\alpha_A/\alpha_B/\alpha_C = 8/4/1$ case indeed gives the worst-case scenario if T_1 is used for control as indicated by traveling distance in Figure 9B. Actually, this can be foreseen by qualitative arguments, but it is reconfirmed here.

3.2.2. Validation using Dynamic Simulation. Dynamic simulation using $T_{sensitive}$ and T_1 as temperature-control trays was carried out for all cases. First, we look at the case of changing relative volatility between LK/HK. The results show that, for the T_1 temperature control, the case of $\alpha_A/\alpha_B/\alpha_C = 3/2/1$ takes a rather long time to reach the final steady-state profile, as compared to the case of $\alpha_A/\alpha_B/\alpha_C = 4/2/1$. The

Figure 10. Reshaping composition profile for T_1 control with -10% Z_B/Z_C for different α_B/α_C: (A) $\alpha_A/\alpha_B/\alpha_C = 3/1.5/1$, (B) $\alpha_A/\alpha_B/\alpha_C = 4/2/1$, and (C) $\alpha_A/\alpha_B/\alpha_C = 8/4/1$.

Table 3. Steady-State Operating Conditions for Different Feed Conditions

	base case	$Z_A = 0.9$	$Z_A = 0.1$
$\alpha_A/\alpha_B/\alpha_C$	4/2/1	4/2/1	4/2/1
F (mol/h)	45.4	45.4	45.4
R (mol/h)	49.5	36.7	50.8
RR	2.15	0.89	11.16
B (mol/h)	22.3	4.1	40.8
D (mol/h)	23.1	41.2	4.6
V (mol/h)	72.7	77.9	55.4
N_T/N_F	25/18	29/25	22/13
β (s)	3.2	3.3	2.6
$M_B/M_D/M_N$ (mol)	17.44/13.34/0.59	15.07/14.31/0.632	17.67/10.17/0.46
$Z_A/Z_B/Z_C$ (m.f.)	0.5/0.256/0.244	0.9/0.056/0.046	0.1/0.449/0.451
$X_{D,A}/X_{D,B}/X_{D,C}$ (m.f.)	0.982/0.0175/0.0005	0.9895/0.01/0.0001	0.9833/0.0166/0.0001
$X_{B,A}/X_{B,B}/X_{B,C}$ (m.f.)	0.001/0.503/0.496	0.0024/0.491/0.5066	0.0014/0.4975/0.501
$A_A/A_B/A_C/B^a$	15.2/14.5/13.8/$-$2768.6	15.2/14.5/13.8/$-$2768.6	15.2/14.5/13.8/$-$2768.6
normal B.P. (K) (A/B/C)	323.2/351.6/385.5	323.2/351.6/385.5	323.2/351.6/385.5

^{a} $\ln P_i^{\text{sat}} = A_{\text{vp},i} + (B_{\text{vp}})/(T)$, where T is in Kelvin.

situation improves a little for the case of $\alpha_A/\alpha_B/\alpha_C = 8/2/1$. On the other hand, when the most sensitive temperature-control tray is selected, we have approximately the same speed of response for all three cases. Note that here we only show the results for the Z_B/Z_C disturbance. Similar results can be found for the other two disturbances (Z_A and F). Next, the case of changing relative volatility between HK/HHK is studied. Figure 10 (parts A−C) shows the traveling distance for each tray, and as predicted, the case of $\alpha_A/\alpha_B/\alpha_C = 8/4/1$ gives the largest traveling distance. Note that here we only show the results for the Z_B/Z_C disturbance. Similar results can be found for the other two disturbances (Z_A and F).

3.3. Summaries. The conflict between process and control directions will become more severe for the following cases: (1) the relative volatility between LK/HK decreases and (2) the relative volatility between the HK/HHK increases. The results can be visualized in the composition space or can be computed quantitatively using the traveling distance. The result is confirmed via rigorous nonlinear dynamic simulation. Qualitatively, the "control" direction is indicated by the isotherm as indicated by the straight lines in Figure 8, and the "process" direction toward the bottoms product end is along the B−C edge. In other words, from the process perspective, we would like to keep impurity level (composition of A) under control (thus, on the B−C edge). Thus, the angle between these two directions can be interpreted as the mismatches between them.[13] The two more severe cases reveal larger mismatches in these directions (e.g., $\alpha_A/\alpha_B/\alpha_C = 3/2/1$ and $\alpha_A/\alpha_B/\alpha_C = 8/4/1$ give the smallest slopes in the corresponding categories, while the process direction gives a slope approaching infinity). Even simpler, in terms of the composition profile, these worst cases have the largest maximum X_B composition (most severe wrong way behavior in X_B, as shown in Figure 8).

4. Effect of Feed Conditions

4.1. Steady-State Process Description. Here we look at what happens when we change the feed composition. Three cases are considered:

- $Z_A = 0.5$: base case
- $Z_A = 0.1$: less light component
- $Z_A = 0.9$: more light component

Distillation columns are designed for each feed composition, and Table 3 gives the steady-state operating conditions for all three cases. Figure 11 shows the composition profiles. The results show that, as the light component decreases in the feed, the composition profile moves closer to the Z_B-Z_C edge, where we lose a degree of freedom. It is expected that the selection of the temperature-control tray will be crucial when Z_A decreases.

4.2. Dynamics. Temperature-control trays are selected according to a sensitivity analysis. The results are as follows:

- $Z_A = 0.1$: T_{16} (selected by most sensitive tray)
- $Z_A = 0.5$: T_{10} (selected by most sensitive tray)
- $Z_A = 0.9$: T_7 (selected by most sensitive tray)

Note that, for $Z_A = 0.1$, the most sensitive temperature-control tray is located in the rectifying section (above the feed point), which is not a typical location for controlling the impurity in the bottom.

4.2.1. Traveling Distance for Different Feed Conditions. The traveling distances are computed for the Z_B/Z_C disturbance for all three cases. The results (Figure 12) show that it is important to select the right temperature-control tray, especially when we try to control the composition close to the edge.

4.2.2. Validation using Dynamic Simulation. The results of dynamic simulation reveal significant traveling distances, and slower dynamics, as the light component (A) feed composition decreases (e.g., $Z_A = 0.1$) when T_1 is under control (Lin).[16] It
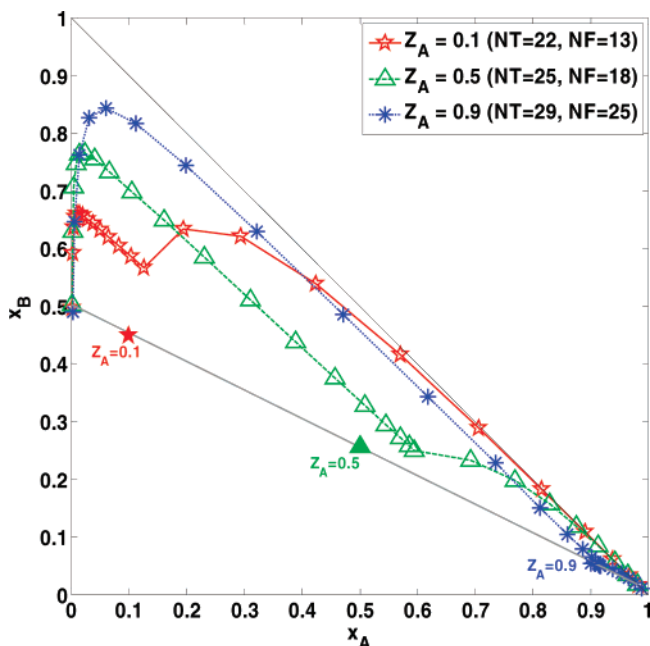
Figure 11. Composition profiles for different feed conditions with straight line indicating material balance line with corresponding feed composition, Z_A.
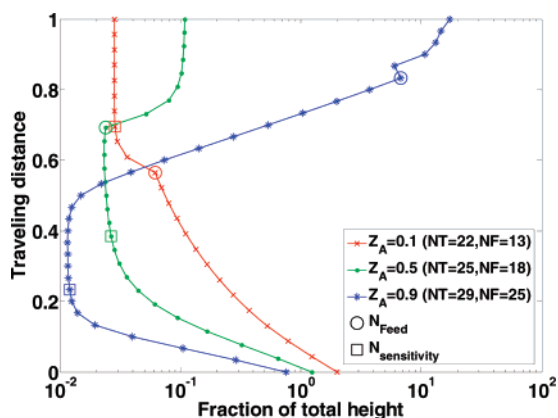

Figure 12. Traveling distance for Z_B/Z_C change with different feed conditions. (Note: fractions 0 and 1 correspond to the bottom and top of the column, respectively.)

also shows that a small tray composition redistribution occurs when the most sensitive temperature-control tray is held constant. Similar results have also been found for the Z_B/Z_C disturbance, with a larger traveling distance for the case of Z_A = 0.1.

4.3. Summary. The results presented here clearly show that the large traveling distances resulting from the loss of a degree of freedom and the conflict between process and control directions also apply to different feed conditions. It is important to select the appropriate temperature-control tray to avoid a large traveling distance. When the light component in the feed decreases, the conflict amplifies.

5. Indirect Split

5.1. Process Description. Can the same analysis be carried over to the indirect separation mode? Here we have a column with $Z_A = Z_B = 0.25$ and $Z_C = 0.5$, in which pure C (~0.98) is withdrawn from the bottom and the mixture of A and B is taken out from the top with C as the distillate impurity. Table 4 gives the steady-state operating conditions. Toward the column top, we have a loss of a degree of freedom when the separation
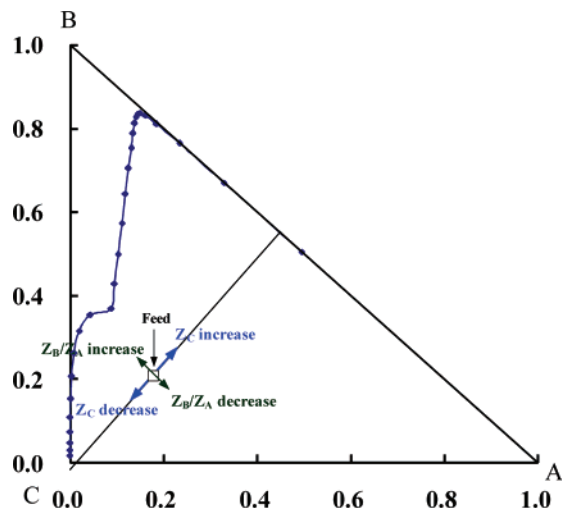

Figure 13. Feed and composition profile for the indirect separation system.
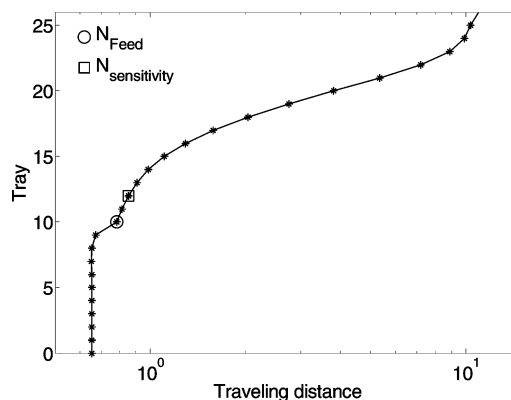

Figure 14. Traveling distance for Z_B/Z_A change with indirect separation.

Table 4. Steady-State Operating Condition for Indirect Separation

	indirect separation
$\alpha_A/\alpha_B/\alpha_C$	4/2/1
F (mol/h)	45.4
R (mol/h)	51.6
RR	2.313859
B (mol/h)	22.3
D (mol/h)	73.9
V (mol/h)	45.4
N_T/N_F	25/10
β (s)	3.2
$M_B/M_D/M_N$ (mol)	8.1/6.2/0.3
$Z_A/Z_B/Z_C$ (m.f.)	0.2436/0.2564/0.5
$X_{D,A}/X_{D,B}/X_{D,C}$ (m.f.)	0.4956/0.5039/0.0005
$X_{B,A}/X_{B,B}/X_{B,C}$ (m.f.)	0.00006/0.0171/0.98284
$A_A/A_B/A_C/B^a$	15.2/14.5/13.8/−2768.6
normal B.P. (K) (A/B/C)	323.2/351.6 /385.5

^{a} $\ln P_i^{sat} = A_{vp,i} + (B_{vp})/(T)$, where T is in Kelvin.

is performed between A and B with almost no C. In a sense, this can be viewed as a mirror image of the direct separation. Figure 13 shows the composition profile.

5.2. Dynamics. 5.2.1. Traveling Distance for Indirect Separation. Traveling distance can be computed from steady-state gain matrices, for any given disturbance. Dynamic simulations were also carried out using the most sensitive temperature for control (T_{12}) and the top tray (T_{25}) as temperature-control trays for the three top purity levels. The figures clearly show that the traveling distance increases significantly when T_{25} is under control (Figure 14) for Z_B/Z_A disturbance. Slow dynamics is expected for T_{25} temperature control, while good control will be achieved using T_{12} temperature control.

5.2.2. Validation using Dynamic Simulation. Dynamic simulations using T_{12} and T_{25} as temperature-control trays were carried out for three disturbances (F, Z_C, Z_B/Z_A changes). For a -20% F change, the case of T_{25} temperature control takes a longer time to reach the final steady-state profile as compared with T_{12} temperature control. This is also true for the Z_B/Z_A disturbance.

5.3. Summary. The indirect split shows the mirror image of the direct split, and the same arguments apply about the loss of a degree of freedom plus the conflict between process and control directions.

6. Conclusions

This paper explores potential problems of temperature-control locations in multicomponent distillation columns. Explanations of the problem are given with different levels of complexity. Qualitatively, we experience a potential conflict between the process and control directions, which can be visualized in the triangular composition space. The situation is worsened when we have a loss of a degree of freedom as the composition profile travels along one of the sides of the triangle. Quantitatively, the traveling distance can be computed, and the potential dynamic problem can be seen directly. Rigorous dynamic simulations are carried out to validate the results. These principles apply to various conditions, and we explore the severity for different situations. For the *direct* separation between A(LK), B(HK), and C (HHK) with a high purity of A at the top, the results are as follows: (1) the conflict between process and control directions becomes more severe as the product purity increases; (2) the conflict between process and control directions becomes worse as the separation between light and heavy key components becomes more difficult; (3) the conflict between process and control directions deteriorates as the separation between heavy and heavier-than-heavy key components becomes easier; and (4) the conflict worsens as the feed composition of the light component decreases. The results can be translated over to the *indirect* separation between A(LLK), B(LK), and C (HK) with a high purity of C on the bottom, while substituting heavy for light in the above principles.

Nomenclature

$A_{vp,i}$ = Antoine coefficient for component i
B_{vp} = Antoine coefficient (same for all components)
B = bottoms flow rate, mol/h
D = distillate flow rate, mol/h
d = load variable representing F, Z_A, or Z_B/Z_C changes
F = feed flow rate, mol/h
$G_{j,i}^{(k)}$ = process transfer function of component i of the jth tray ($x_{j,i}$) under the kth manipulated variable (u_k)
$G_{Lj,i}$ = load transfer function of component i of the jth tray ($x_{j,i}$) under load variable d
$G_{Tj}^{(k)}$ = process transfer function of the temperature of the jth tray (T_j) under the kth manipulated variable (u_k)
G_{LTj} = load transfer function of the temperature of the jth tray (T_j) under load variable d
M_B = liquid holdup of bottoms base, mol
M_D = liquid holdup of reflux drum, mol
M_N = liquid holdup of each tray, mol
NT = total number of trays

NF = feed location
P_i^{sat} = vapor pressure of component i
R = reflux flow rate, mol/h
RR = reflux ratio (R/D)
T_j = jth tray temperature, K
u = manipulated variable
V = vapor boilup rate, mol/h
x_i = liquid-phase composition of the ith component, m.f.
$x_{j,i}$ = ith component liquid-phase composition on the jth tray, m.f.
$X_{B,i}$ = bottoms composition of the ith component, m.f.
$X_{D,i}$ = distillate composition of the ith component, m.f.
y_i = vapor-phase composition of the ith component, m.f.
Z_i = feed composition of the ith component, m.f.

Greek Symbols

α_i = relative volatility of component i
β = liquid hydraulic time constant, s

Literature Cited

(1) Lin, M. T.; Yu, C. C.; Luyben, M. L. Interpretation of temperature control for ternary distillation. *Ind. Eng. Chem. Res.* **2005**, *44*, 8277−8290.

(2) Yu, C. C.; Luyben, W. L. Control of multicomponent distillation columns using rigorous composition estimators. *Inst. Chem. Eng. Symp. Ser.* **1989**, *104*, A29−A69.

(3) Mejdell, T.; Skogestad, S. Estimation of distillation compositions from multiple temperature measurements using partial least-squares regression. *Ind. Eng. Chem. Res.* **1991**, *30*, 2543−2555.

(4) Baratti, R.; Bertucco, A.; Da Rold, A.; Morbidelli, M. A composition estimator for multicomponent distillation columns−Development and experimental tests on ternary mixtures. *Chem. Eng. Sci.* **1998**, *53*, 3601−3612.

(5) Kano, M.; Miyazaki, K.; Hasebe, S.; Hashimoto, I. Inferential control system of distillation compositions using dynamic partial least squares regression. *J. Process Control* **2000**, *10*, 157−166.

(6) Pannocchia, G.; Brambilla, A. Consistency of property estimators in multicomponent distillation control. *Ind. Eng. Chem. Res.* **2003**, *42*, 4452−4460.

(7) Tronci, S.; Bezzo, F.; Barolo, M.; Barolo, R. Geometric observer for a distillation column: Development and experimental testing. *Ind. Eng. Chem. Res.* **2005**, *44*, 9884−9893.

(8) Luyben, W. L. Guides for the Selection of Control Structures for Ternary Distillation Columns. *Ind. Eng. Chem. Res.* **2005**, *44*, 7113−7119.

(9) Luyben, W. L. Evaluation of criteria for selecting temperature control trays in distillation columns. *J. Process Control* **2006**, *16*, 115−134.

(10) Hori, E. S.; Skogestad, S. Selection of control structure and temperature location for two-product distillation columns. *Chem. Eng. Res. Des.* **2007**, *85*, 293−306.

(11) Castellanos-Sahagun, E.; Alvarez-Ramirez, J.; Alvarez, J. Two-point composition−temperature control of binary distillation columns. *Ind. Eng. Chem. Res.* **2006**, *45*, 9010−9023.

(12) Chien, I. L.; Ogunnaike, B. A. Modeling and control of a temperature-based high-purity distillation column. *Chem. Eng. Commun.* **1997**, *158*, 71−105.

(13) Fuentes, C.; Luyben, W. L. Control of high-purity distillation columns. *Ind. Eng. Chem. Process Des. Dev.* **1983**, *22*, 361−366.

(14) Wang, S. J.; Yu, S. W. Nonlinear control of a high-purity distillation column. *J. Chin. Inst. Chem. Eng.* **1998**, *29*, 183−192.

(15) Zhu, Y.; Liu, X. G. Dynamics and control of high purity heat integrated distillation columns. *Ind. Eng. Chem. Res.* **2005**, *44*, 8806−8814.

(16) Lin, M. T. Interpretation of temperature control for multicomponent distillation. MS Thesis, National Taiwan University, Taipei, Taiwan, 2004.